How to cite: *Angew. Chem. Int. Ed.* **2022,** *61,* e202209335
International Edition: doi.org/10.1002/anie.202209335
German Edition: doi.org/10.1002/ange.202209335

MOFs Hot Paper

Framework Adaptability and Concerted Structural Response in a Bismuth Metal-Organic Framework Catalyst.

Eloy P. Gómez-Oliveira, Daniel Reinares-Fisac, Lina M. Aguirre-Díaz, Fátima Esteban-Betegón, Mercedes Pintado-Sierra, Enrique Gutiérrez-Puebla, Marta Iglesias, M. Ángeles Monge, and Felipe Gándara**

Abstract: Bismuth metal–organic frameworks (MOFs) as heterogeneous catalysts are scarce, and there is little knowledge on the influence of the MOF features on their resulting activity and behavior. Here, we present the synthesis, characterization, and catalytic activity in the one-pot multicomponent Strecker reaction with ketones of three new MOFs prepared with the combination of indium or bismuth and 4,4′,4″,4‴-methanetetrayltetrabenzoic acid. One of them, denoted BiPF-7, is very robust and chemically stable, and demonstrates a high activity in the formation of the desired α-aminonitriles. The interaction of the catalytic substrates with the metal centers in this MOF has been crystallographically characterized, showcasing a concerted framework adaptability process that involves structural changes in framework components that are not directly involved in the binding of the guests.

Introduction

Metal-organic frameworks, MOFs, are a class of reticular materials built up by the combination of metal elements and organic linkers, with periodic, extended structures.[1] During the past two decades, MOFs have found numerous applications in a number of different fields. Among them, the use of MOFs as heterogeneous catalysts is one of the most extensively studied application.[2–7] As such, different strategies are followed to exploit MOFs' characteristics to design novel catalysts for countless reactions. Thus, by taking advantage of their porosity and high surface area, MOFs offer the possibility to incorporate large number of accessible catalytically active species in their structures,[8–10] or to include specific organic linkers judiciously selected or modified to display active sites accessible through the pores.[11] Nevertheless, the rational choice of the metal elements that constitute the secondary building units (SBU)[12] continues to be a very versatile approach to design and create novel active MOF heterogeneous catalysts.[13] In this category, metal elements with Lewis acid character are often used to build up the inorganic SBUs,[14] providing the structures with accessible active sites. Among the different elements falling in this category, indium is of great interest, because it is a non-toxic element with a strong Lewis acid character. Thus, over the years, our group and others have developed several MOF families based on the use of indium as metal element,[15–24] and demonstrated that they are indeed highly active catalysts for a range of different transformations,[25] including the multicomponent Strecker reaction.[26–28] Recently, we have also turned our attention to the use of another main group element, bismuth, to synthesize novel catalytically active MOFs with this metal.[29] Bismuth is also an element of low-toxicity, it is unexpensive and highly earth-abundant. In recent years an increasing number of new MOFs have appeared in the literature with the use of bismuth as element of choice in the formation of the inorganic SBUs, some of them showing outstanding potential in multiple fields.[30–39] Thus, a number of bismuth MOFs have been reported with the use of linkers commonly employed in MOF chemistry.[34,40] However, and despite the increasing number of new bismuth MOFs, the use of this element to obtain robust and chemically stable compounds still poses a synthetic challenge, arguably arising from its large and variable coordination number, as well as from its tendency to hydrolyzation. The use of robust bismuth MOFs as heterogeneous Lewis acid catalyst is therefore very attractive, provided that the synthesized materials reach competitive performance in terms of activity, selectivity, and recyclability, as compared to MOFs prepared with other, more widely explored metal elements.

With this motivation, here we present the synthesis, crystal structure, characterization, and catalytic activity of a

[*] E. P. Gómez-Oliveira, Dr. D. Reinares-Fisac, Dr. L. M. Aguirre-Díaz, Dr. F. Esteban-Betegón, Prof. E. Gutiérrez-Puebla, Dr. M. Iglesias, Prof. M. Ángeles Monge, Dr. F. Gándara
Materials Science Institute of Madrid, ICMM, Spanish National Research Council, CSIC
Sor Juana Inés de la Cruz, 3, 28049 Madrid (Spain)
E-mail: amonge@icmm.csic.es
gandara@icmm.csic.es
Dr. M. Pintado-Sierra
General Organic Chemistry Institute, IQOG, Spanish National Research Council, CSIC
C/ Juan de la Cierva, 3, 28006 Madrid (Spain)

© 2022 The Authors. Angewandte Chemie International Edition published by Wiley-VCH GmbH. This is an open access article under the terms of the Creative Commons Attribution Non-Commercial NoDerivs License, which permits use and distribution in any medium, provided the original work is properly cited, the use is non-commercial and no modifications or adaptations are made.

series of MOFs constructed with the use of the tetrahedrally shaped organic linker, 4,4′,4″,4‴-methanetetrayltetrabenzoic acid (H_4MTBA), scheme 1. One of these new materials, denoted InPF-60, has been synthesized with the use of indium as metal center, while bismuth has been the metal of choice in the two others compounds, denoted BiPF-5 and BiPF-7. Despite InPF-60 and BiPF-5 are isoreticular compounds, having the same **dia-c** topology, only InPF-60 is structurally robust under catalytic conditions. Furthermore, BiPF-7 owns a completely different crystal structure with a new topology, and our crystallographic study with single crystal X-ray diffraction data demonstrates the interaction of the catalytic substrate with bismuth atoms, and unveils an unusual example of framework adaptability through the concerted response of various framework components.

Results and Discussion

InPF-60 crystallizes in the monoclinic space group *Cc*, with cell parameters $a=21.3537(10)$ Å, $b=14.9688(6)$ Å, $c=15.0505(7)$ Å, $\beta=132.912°$, and BiPF-5 in the orthorhombic *Pnna* space group, with cell parameters $a=28.0290(15)$ Å, $b=18.5193(8)$ Å, $c=15.0920(7)$ Å. Both MOFs are isoreticular, with structures formed by inorganic SBUs consisting of one metal atom coordinated to four carboxylic acid groups, giving rise to two-fold interpenetrated **dia** networks (Figure 1). The frameworks are negatively charged, and dimethylammonium cations formed by decomposition of DMF solvent during the MOF synthesis are located inside the pores balancing the charge. Despite being isoreticular compounds, we found that, as opposed to InPF-60, the structure of BiPF-5 is not retained under the conditions employed for catalytic activity tests, indicating that this SBU type is not appropriate to create robust bismuth MOFs.

BiPF-7 crystallizes in the rhombohedral *R*-3*c* space group, with cell parameters $a=39.4805(13)$ Å, $c=24.6270(10)$ Å. The structure of BiPF-7 is significantly different from BiPF-5. First of all, there are two different inorganic SBUs (Figure 2). Both of them are composed of two bismuth atoms and six carboxylate groups. In the first one, the bismuth atoms are found with coordination number eight, with bond lengths ranging from 2.231(7) Å to 2.807(6) Å. A coordinated water ligand completes the coordination environment of the bismuth atom. Two out of the six carboxylate groups bridge the two bismuth cations through a shared oxygen atom. In the second inorganic SBU, there are also two bismuth atoms and six carboxylate groups.

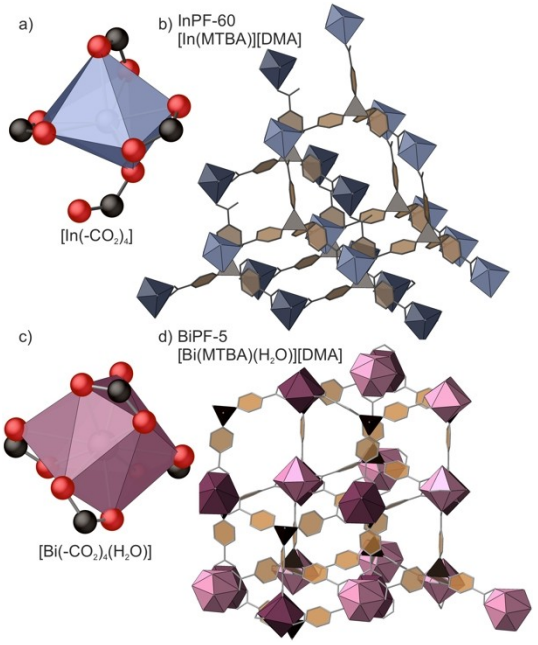

Figure 1. a) The inorganic SBU in InPF-60 is composed of one metal atom coordinated to four carboxylic groups. b) Structural representation of InPF-60. c) The inorganic SBU in BiPF-5, composed of one metal atom coordinated to four carboxylic groups and a water ligand. d) Structural representation of BiPF-5. The central C atom of the organic linker is represented as a black tetrahedron in (b) and (d), while blue and magenta polyhedra represent indium and bismuth atoms, respectively. In both cases, hydrogen atoms and counter-cations are omitted for clarity.

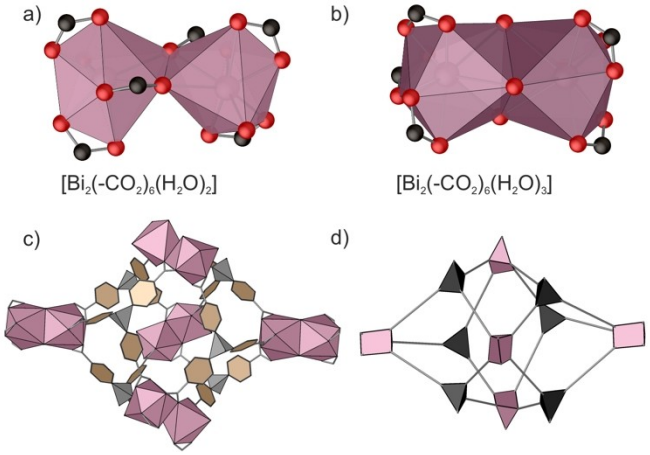

Figure 2. There are two different types of SBUs in the structure of BiPF-7, consisting of two bismuth atoms with bridging carboxylate groups (a), or water ligands (b). Magenta polyhedral, black and red spheres represent bismuth, carbon, and oxygen atoms, respectively. Polyhedral representation of the mtq cage type present in the structure (c), and its simplified view (d), where the inorganic SBUs are shown as trigonal prisms, and the central atom of the organic linker is shown as a black tetrahedron.

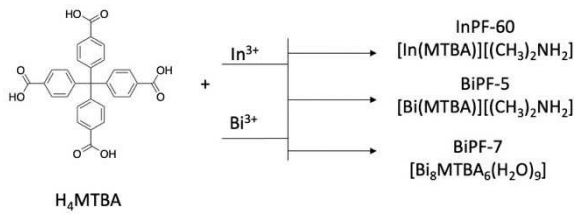

Scheme 1. The organic linker 4,4′,4″,4‴-methanetetrayltetrabenzoic acid in combination with indium or bismuth results in three new MOFs.

© 2022 The Authors. Angewandte Chemie International Edition published by Wiley-VCH GmbH

However, the two bismuth atoms are now bridged by three water ligands. The Bi–O distances range from 2.264(3) Å to 2.967(1) Å, where the longest distance corresponds to the three bridging water oxygen atoms. BiPF-7 has a charge-neutral framework, and therefore there is no presence of charged species in the pores, and only solvent water molecules were located in the electron density maps, at typical hydrogen bond lengths. The two types of six-connected SBUs have a 3:1 stoichiometry, and they are connected through the MTBA linkers to form a three-dimensional framework with a new 4,6-connected topology [point symbol: $(4^4.6^2)_6(4^6.6^6.8^3)_3(4^6.8^6.10^3)$], where the inorganic SBUs have trigonal prismatic shape, and the organic linker has distorted tetrahedral shape. In this new type of network, cages with the shape of **mtq** (Edshammer) type polyhedra[41] are identified, with the inorganic SBUs and the central carbon atom of the organic linker at the vertices, and the linker phenyl rings at the edges (Figure 2). The cages are not isolated, and instead they share vertices to form chains along the [001] direction. Moreover, each one of these chains is catenated by another one symmetrically generated (Figure 3). These catenated pairs of chains are connected among each other to form a self-catenated, three-dimensional network. It has to be noted that the connection between different sets of catenated chains takes place in such a way that it results in just one single self-catenated framework, rather than in the formation of interpenetrated networks.

The three new MOFs were obtained as pure phase, as evidenced by the experimental powder X-ray diffraction patterns (Figures S3.1, S3.4, S3.5), which are coincident with the ones calculated from the single crystal data. The permanent porosity of the activated samples was evaluated with N_2 and CO_2 sorption isotherms collected at 77 K and 273 K, respectively. In the case of InPF-60, the N_2 isotherm curve (Figure S6.1) is indicative of presence of microporosity, with a calculated Brunauer–Emmett–Teller (BET) surface area of 370 $m^2 g^{-1}$. Interestingly, the presence of hysteresis was observed during the desorption cycle. Considering the crystallographically determined pore dimensions, this hysteresis loop should be attributed to certain guest-induced framework flexibility,[42] rather than to presence of mesopores. Indeed, the PXRD pattern collected for the sample after a heating treatment at 125 °C shows that the MOF undergoes a crystal phase transition. This change occurs gradually, with appearance of additional diffraction peaks after 1 d heating, and full conversion after 3 d (Figure S3.2). Consequently, the crystalline transition could not be monitored with SCXR due to the loss of diffracting quality of the single crystals during the process. Nonetheless, the new PXRD pattern was indexed with a *C* centered monoclinic unit cell with parameters $a = 15.30$ Å, $b = 23.96$ Å, $c = 11.68$ Å, $\beta = 129.05°$ (see Figure S3.3 for the corresponding profile fitting). The volume of the new cell is 3327 $Å^3$, which implies a contraction of the cell, as compared to the original volume of 3518 $Å^3$. The N_2 sorption isotherm of BiPF-5 (Figure S6.1) shows moderate uptake at low relative pressures, indicating limited accessibility to the micropores (BET area 135 $m^2 g^{-1}$), followed by a constant rise in the uptake with increasing relative pressure. It should be noted that both InPF-60 and BiPF-5 contain cationic species in their pores to compensate the negative charge of the frameworks. This fact, along with their framework interpenetration degree possibly explains the unusual sorption profiles for these two materials. On the contrary, the neutral compound BiPF-7 shows a type I isotherm profile expected for a microporous sample, with a BET surface area

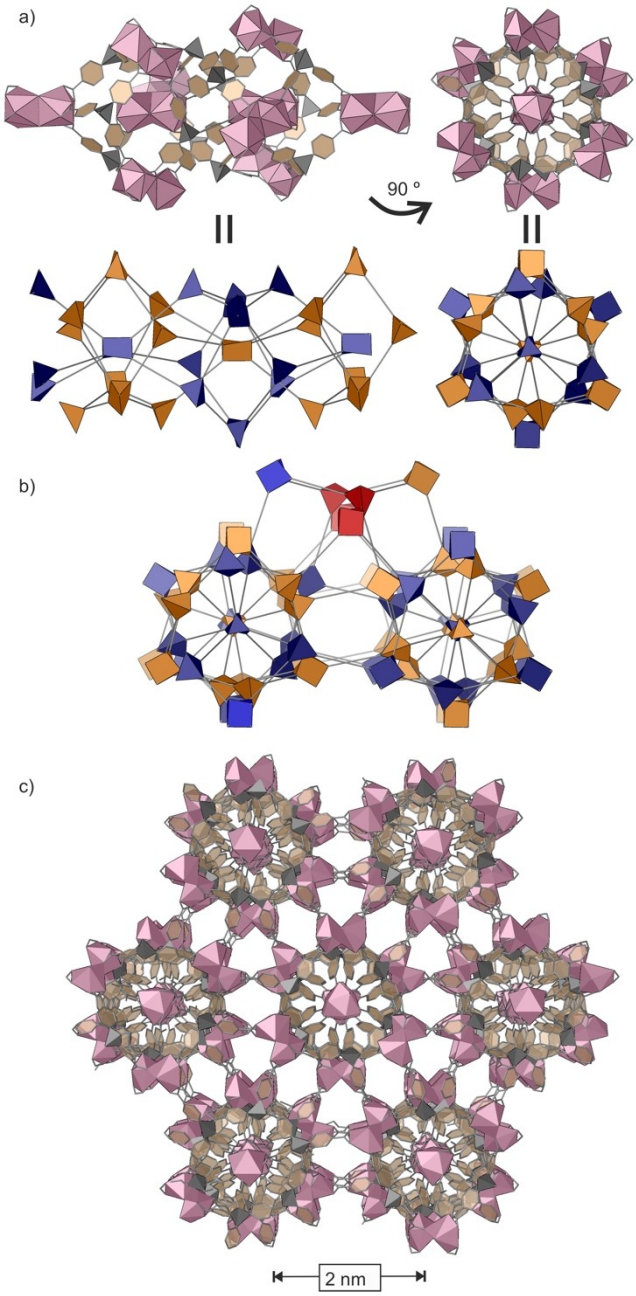

Figure 3. a) The structure of BiPF-7 is composed of vertex-sharing cages that extend along the [001] direction. In the simplified view, two sets of catenated chains are represented in orange and blue color. b) Pairs of catenated chains are connected at the positions highlighted in red, resulting in the formation of a single, self-catenated three-dimensional framework (c).

© 2022 The Authors. Angewandte Chemie International Edition published by Wiley-VCH GmbH

of 425 $m^2 g^{-1}$. In addition, all three compounds are able to adsorb carbon dioxide, with a maximum uptake of 1.2, 0.97, and 2.5 $mmol g^{-1}$ at 1 atm and 273 K, for InPF-60, BiPF-5, and BiPF-7, respectively (Figures S6.3–S6.5).

At the view of the structural features for these new MOFs, we evaluated their activity as heterogeneous catalysts in the one-pot three-component Strecker reaction of ketones with aliphatic or aromatic amines and trimethylsilyl cyanide to obtain α-aminonitriles. Most of the reported examples of Strecker reaction include aldehydes as substrates, and the reaction applied to ketones and aliphatic amines remains a more demanding process. The use of MOFs with presence of Lewis acid sites as heterogeneous catalysts for this reaction has been previously investigated,[28] with several indium MOFs showing excellent performance in terms of activity and selectivity.[26] In the case of bismuth, some MOFs have been reported exhibiting catalytic activity,[36,43] and their Lewis acid character has been tested in reactions such as the ring-opening of styrene oxide to 2-methoxy-2-phenylethanol.[44] However, the use of bismuth compounds as heterogeneous catalysts for the one-pot multicomponent Strecker reaction has not been investigated yet. We therefore started by testing the catalytic activity of InPF-60 with the use of acetophenone, aniline, and trimethylsilyl cyanide (TMSCN) as model substrates. Catalytic amounts (1 mol % based on metal atoms) of the MOFs were placed in a Schlenk tube, followed by the addition of the three reactants. The reactions were performed at room temperature under solvent-free conditions. InPF-60 demonstrated very high activity, and after 4 h a 95 % conversion was achieved, with 99 % selectivity towards the α-aminonitrile product. However, when BiPF-5 was used as catalyst under the same reaction conditions (r.t., solvent free, 1 mol %, 4 h), we found that it significantly loses crystallinity after reaction, indicating a framework collapse, and therefore, it was discarded for further study. On the contrary, BiPF-7 demonstrated a superior performance, which is comparable to InPF-60, reaching 97 % conversion and 99 % selectivity to the Strecker product. Under the standard conditions of 1 mol % catalyst loading, room temperature and 4 h of reaction time, we explored the activity of InPF-60 and BiPF-7 in the three-component reaction with several aromatic and aliphatic ketones and anilines with different functional groups and TMSCN. Thus, InPF-60 shows good activity and selectivity towards the synthesis of α-aminonitriles with several substituted ketones (Scheme 2). Aromatic ketones with electron donor groups such as 4-methylacetophenone, resulted in high conversion of acetophenone to give the corresponding α-amino nitrile. On the contrary, 4-chloroacetophenone only yields traces of the product. The aliphatic ketone also results in high yield and selectivity for the resultant nitrile.

Reaction of acetophenone with substituted anilines and n-butylamine yields selectively the corresponding cyanosilylated product. BiPF-7 afforded the Strecker product for various substituted amines and ketones, with exception of p-anisidine, and n-butylamine, for which only cyanosilylation products were detected (Table S8.2). The reusability of these two catalysts was tested by performing up to 9

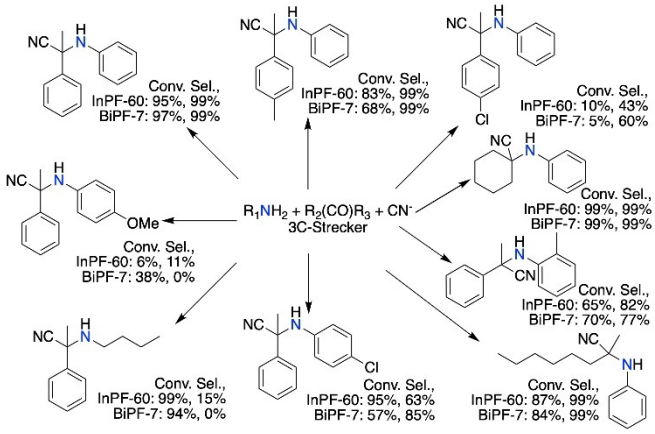

Scheme 2. Summary of the Strecker products obtained with the use of InPF-60 and BiPF-7 catalysts.

consecutive reaction cycles with the model reaction between acetophenone, aniline and TMSCN. No significant decrease in conversion was observed for any of the MOFs (Figure S9.3). Their structural integrity was then checked with the collection of a PXRD pattern for the recovered catalysts after each reaction cycle. Both InPF-60 and BiPF-7 fully retain their crystallinity, with no significant changes in their corresponding PXRD patterns, demonstrating their robustness under reaction conditions

The one-pot formation of the corresponding Strecker products is probably completed by following the proposed reaction mechanism that involves the formation of the imine intermediate followed by addition of the cyanide reactant.[45,46] To gain further structural insights on the response of the framework during the interaction with the employed catalytic substrates, we completed additional X-ray diffraction experiments with BiPF-7 crystals after being exposed to the selected molecules employed in the model Strecker reaction. Thus, crystals of BiPF-7 were immersed for 24 h in aniline, acetophenone, and a 1:1 mixture of them, followed by the acquisition of the corresponding single-crystal X-ray diffraction data. Starting with BiPF-7_aniline crystal, after data analysis we first noticed an expansion of the unit cell volume, from 33244(3) $Å^3$ to 36184(16) $Å^3$. The structure could be solved and refined in the same *R*-3*c* space group. Remarkably, several differences were observed as compared to the pristine crystals, particularly in the inorganic SBUs. Thus, the $[Bi_2(\text{-}CO_2)_6(H_2O)_3]$ SBU is now split in two $[Bi(\text{-}CO_2)_3]$ units (Figure 4). The coordinated water ligands are no longer bridging the metal atoms, and the bismuth centers have moved apart one from each other, from 4.387 Å to 5.294 Å. Additional electron density was found in the vicinity of this SBU. However, no clear position corresponding to any aniline molecule could be deduced. This is not surprising, considering the size of the window where aniline molecules would need to diffuse through for accessing the metal centers. This residual density is thus attributed to additional, disordered water molecules, which were already present in the as-synthesized MOF. More subtle changes were detected regarding the [Bi_2(-

© 2022 The Authors. Angewandte Chemie International Edition published by Wiley-VCH GmbH

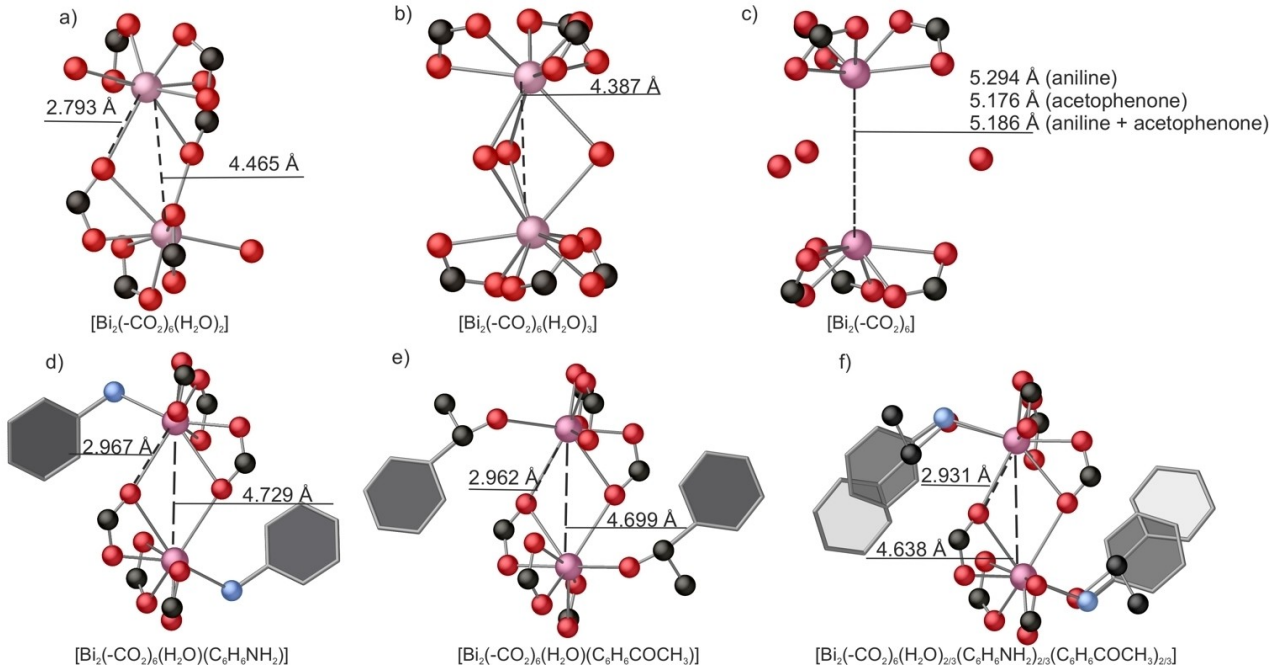

Figure 4. Differences in bond lengths are evidenced in both types of SBUs. Figures a) and b) correspond to the two types of SBU in the as-synthesized crystals. Upon exposure to the substrates, a marked change in the Bi–Bi distance is resulted in one of the inorganic SBUs (c), whereas the guest molecules, including aniline (d), acetophenone (e), and mixture of them (f), interact with bismuth atoms in the other SBU type. Magenta, black, red, and blue spheres represent Bi, C, O, and N atoms.

$CO_2)_6(H_2O)_2]$ SBU. The Bi–Bi distance is now longer too, but the variation is smaller than for the previous case, going from 4.465 Å to 4.729 Å. This is consequence of the enlargement of the Bi–O distance corresponding to the bridging carboxylate group, which goes from 2.793 Å to 2.959 Å. Nevertheless, the most evident change is found at the coordination site previously occupied by a water ligand. Two close areas of high electron density are clear now, which were attributed to two atoms with 50 % occupancy. One of them still corresponds to a water ligand previously present, while the other one is assigned to the nitrogen atom of an aniline molecule. Indeed, the carbon atoms from the aniline phenyl ring were located in the difference Fourier maps. Thus, the aniline molecules are coordinatively adsorbed by the MOF, with a Bi–N distance of 2.762 Å, supporting the important role of the inorganic SBU by interacting with the amines during the one-pot multicomponent Strecker reaction. Single crystal diffraction data was also collected for BiPF-7 crystals soaked in acetophenone. Similar changes are also observed regarding the atomic rearrangement of the SBUs, with a Bi–Bi distance of 5.176 Å in the now split SBU. This fact further demonstrates the lability of the water bridges between bismuth atoms, and framework flexibility when in organic medium. In addition, a possible orientation of the acetophenone molecules was identified near the $[Bi_2(-CO_2)_6(H_2O)_2]$ SBU, with a similar approximation to the metal center, by replacing the water ligands. Moreover, when both aniline and acetophenone are present, equivalent positions are identified, with partial occupancies for each one of them (Figure 4f). In all cases, these results show how the presence of the substrates near to one SBU results in a concerted atomic response in the second SBU, where an elongation of the distance between metal atoms, and rearrangement of the water molecules take place. This structural change takes place not only with catalytic substrates, but also with presence of other molecules with ability to interact with the inorganic SBU. In particular, we also collected diffraction data for a crystal immersed in bromobenzene (Table S2.7), finding that this molecule is also adsorbed with the bromine atom in the vicinity of the SBU, triggering the same structural change.

This structural adjustment in one part of the framework in response to the presence and interaction of guest molecules with atoms in different sites (Figure 5) is not commonly found in porous solids. Thus, BiPF-7 can be considered as an exemplar of adaptable material showing a concerted structural response involving binding of guest molecules at binding pockets with specific docking sites at the bismuth atoms and non-bonding interaction with the organic linkers, which triggers the atomic rearrangement in the spatially separated framework building components (Figure 5).

Conclusion

The three new MOFs here disclosed show the marked differences in framework robustness and catalytic activity between indium and bismuth isoreticular MOFs. Thus, while InPF-60 continues to demonstrate the excellent activity and selectivity of indium MOFs for the Strecker reaction of ketones, BiPF-5 shows poor framework stability. However,

© 2022 The Authors. Angewandte Chemie International Edition published by Wiley-VCH GmbH

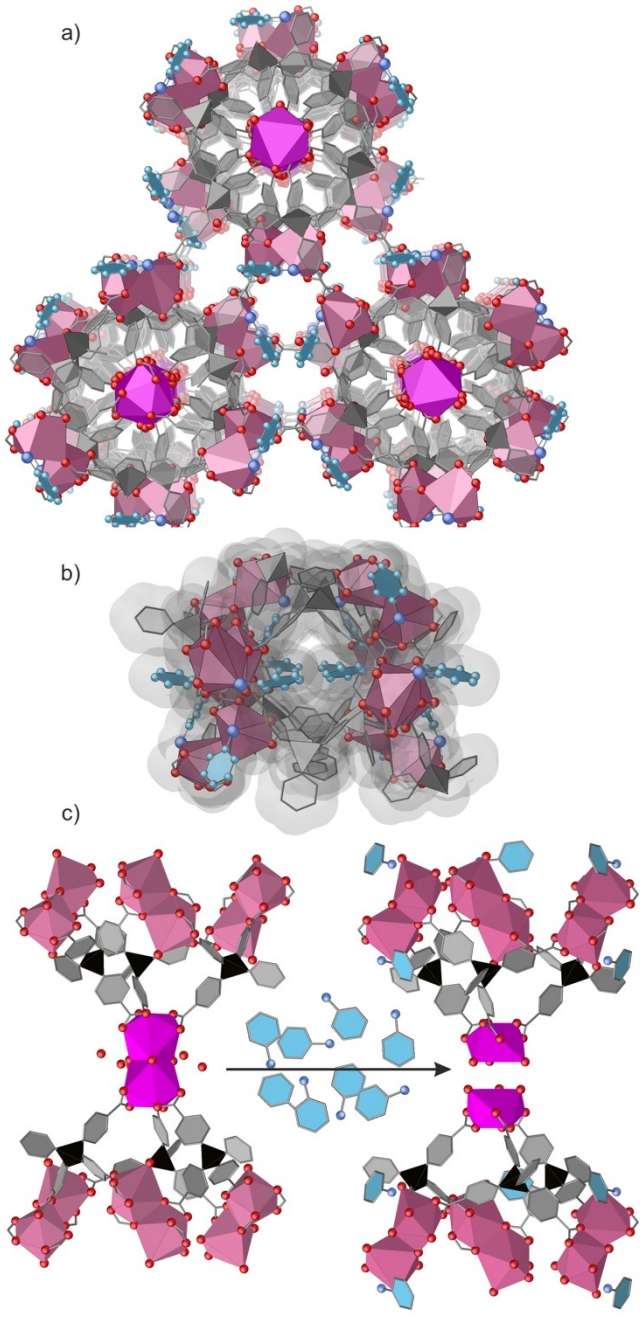

Figure 5. Guest molecules are adsorbed in the accessible pores of BiPF-7 (a). In the figure, the crystallographically located aniline molecules are highlighted with blue color. A zoomed-in view of the sorption pockets is shown in (b), with representation of the corresponding Van der Waals surfaces to illustrate the interactions. The adaptability of BiPF-7 during the uptake of guest molecules is enabled by the structural changes that take place in SBUs (highlighted as purple polyhedra) that are not directly involved in the binding (c).

the potential to use bismuth MOFs as efficient heterogeneous catalysts in this reaction is here demonstrated with BiPF-7. The crystallographic study[47] carried out with this new robust porous material shows not only the central role of the inorganic SBU in the interaction with the catalytic substrate, but also an unusual mechanism of framework adaptability during the reaction. These new findings will serve to further advance the use of a low-toxicity and highly abundant element such as bismuth in the field of reticular chemistry, as well as in the development of materials with concerted structural responses towards presence of guest species.

Acknowledgements

Grant CTQ-2017-87262-R funded by MCIN/AEI/10.13039/501100011033 and by "ERDF A way of making Europe". Grants PID2019-107675-RB-I00 and PID2020-112590GB-C22 funded by MCIN/AEI/10.13039/501100011033. Grant PLEC2021-007906 (SOLFuture) funded by MCIN/AEI/10.13039/501100011033 and by the "European Union Next-GenerationEU/PRTR".

Conflict of Interest

The authors declare no conflict of interest.

Data Availability Statement

The data that support the findings of this study are available in the Supporting Information of this article.

Keywords: Bismuth · Heterogeneous Catalysis · Metal-Organic Frameworks · Strecker Reaction

[1] H. Furukawa, K. E. Cordova, M. O'Keeffe, O. M. Yaghi, *Science* **2013**, *341*, 1230444.
[2] E. Gkaniatsou, C. Sicard, R. Ricoux, J.-P. Mahy, N. Steunou, C. Serre, *Mater. Horiz.* **2017**, *4*, 55–63.
[3] A. Corma, H. García, F. X. Llabrés i Xamena, *Chem. Rev.* **2010**, *110*, 4606–55.
[4] Y.-S. Kang, Y. Lu, K. Chen, Y. Zhao, P. Wang, W.-Y. Sun, *Coord. Chem. Rev.* **2019**, *378*, 262–280.
[5] L. Jiao, Y. Wang, H.-L. Jiang, Q. Xu, *Adv. Mater.* **2018**, *30*, 1703663.
[6] A. Dhakshinamoorthy, Z. Li, H. Garcia, *Chem. Soc. Rev.* **2018**, *47*, 8134–8172.
[7] L. Zeng, X. Guo, C. He, C. Duan, *ACS Catal.* **2016**, *6*, 7935–7947.
[8] X. Fang, Q. Shang, Y. Wang, L. Jiao, T. Yao, Y. Li, Q. Zhang, Y. Luo, H.-L. Jiang, *Adv. Mater.* **2018**, *30*, 1705112.
[9] K. M. Choi, D. Kim, B. Rungtaweevoranit, C. A. Trickett, J. T. D. Barmanbek, A. S. Alshammari, P. Yang, O. M. Yaghi, *J. Am. Chem. Soc.* **2017**, *139*, 356–362.
[10] L. Jiao, H.-L. Jiang, *Chem* **2019**, *5*, 786–804.
[11] A. Broto-Ribas, C. Vignatti, A. Jimenez-Almarza, J. Luis-Barrera, Z. Dolatkhah, F. Gándara, I. Imaz, R. Mas-Ballesté, J. Alemán, D. Maspoch, *Nano Res.* **2021**, *14*, 458–465.
[12] M. J. Kalmutzki, N. Hanikel, O. M. Yaghi, *Sci. Adv.* **2018**, *4*, eaat9180.
[13] B. Li, K. Leng, Y. Zhang, J. J. Dynes, J. Wang, Y. Hu, D. Ma, Z. Shi, L. Zhu, D. Zhang, Y. Sun, M. Chrzanowski, S. Ma, *J. Am. Chem. Soc.* **2015**, *137*, 4243–4248.
[14] Z. Hu, D. Zhao, *CrystEngComm* **2017**, *19*, 4066–4081.

© 2022 The Authors. Angewandte Chemie International Edition published by Wiley-VCH GmbH

[15] Y.-Z. Li, G.-D. Wang, Y.-K. Lu, L. Hou, Y.-Y. Wang, Z. Zhu, *Inorg. Chem.* **2020**, *59*, 15302–15311.
[16] J. Benecke, E. S. Grape, A. Fuß, S. Wöhlbrandt, T. A. Engesser, A. K. Inge, N. Stock, H. Reinsch, *Inorg. Chem.* **2020**, *59*, 9969–9978.
[17] H. Li, M. Liang, W. Sun, Y. Wang, *Adv. Funct. Mater.* **2016**, *26*, 1098–1103.
[18] Q.-G. Zhai, C. Mao, X. Zhao, Q. Lin, F. Bu, X. Chen, X. Bu, P. Feng, *Angew. Chem. Int. Ed.* **2015**, *54*, 7886–7890; *Angew. Chem.* **2015**, *127*, 7997–8001.
[19] Y. Huang, Z. Lin, H. Fu, F. Wang, M. Shen, X. Wang, R. Cao, *ChemSusChem* **2014**, *7*, 2647–2653.
[20] J. Xia, J. Xu, Y. Fan, T. Song, L. Wang, J. Zheng, *Inorg. Chem.* **2014**, *53*, 10024–10026.
[21] T. Panda, T. Kundu, R. Banerjee, *Chem. Commun.* **2013**, *49*, 6197–6199.
[22] L. Sun, H. Xing, Z. Liang, J. Yu, R. Xu, *Chem. Commun.* **2013**, *49*, 11155–11157.
[23] S. Huh, T.-H. Kwon, N. Park, S.-J. Kim, Y. Kim, *Chem. Commun.* **2009**, 4953–4955.
[24] Y. Liu, J. F. Eubank, A. J. Cairns, J. Eckert, V. C. Kravtsov, R. Luebke, M. Eddaoudi, *Angew. Chem. Int. Ed.* **2007**, *46*, 3278–3283; *Angew. Chem.* **2007**, *119*, 3342–3347.
[25] L. M. Aguirre-Díaz, D. Reinares-Fisac, M. Iglesias, E. Gutiérrez-Puebla, F. Gándara, N. Snejko, M. Á. Monge, *Coord. Chem. Rev.* **2017**, *335*, 1–27.
[26] G. Verma, K. Forrest, B. A. Carr, H. Vardhan, J. Ren, T. Pham, B. Space, S. Kumar, S. Ma, *ACS Appl. Mater. Interfaces* **2021**, *13*, 52023–52033.
[27] D. Reinares-Fisac, L. M. Aguirre-Díaz, M. Iglesias, N. Snejko, E. Gutiérrez-Puebla, M. Á. Monge, F. Gándara, *J. Am. Chem. Soc.* **2016**, *138*, 9089–9092.
[28] J. Chai, P. Zhang, J. Xu, H. Qi, J. Sun, S. Jing, X. Chen, Y. Fan, L. Wang, *Inorg. Chim. Acta* **2018**, *479*, 165–171.
[29] A. García-Sánchez, M. Gomez-Mendoza, M. Barawi, I. J. Villar-Garcia, M. Liras, F. Gándara, V. A. de la Peña O'Shea, *J. Am. Chem. Soc.* **2020**, *142*, 318–326.
[30] D. T. Tran, D. Chu, A. G. Oliver, S. R. J. Oliver, *Inorg. Chem. Commun.* **2009**, *12*, 1081–1084.
[31] Y. Q. Sun, S. Z. Ge, Q. Liu, J. C. Zhong, Y. P. Chen, *CrystEngComm* **2013**, *15*, 10188–10192.
[32] S. Li, Y. Zhang, Y. Hu, B. Wang, S. Sun, X. Yang, H. He, *J. Mater.* **2021**, *7*, 1029–1038.
[33] G. E. Gomez, R. F. D'vries, D. F. Lionello, L. M. Aguirre-Díaz, M. Spinosa, C. S. Costa, M. C. Fuertes, R. A. Pizarro, A. M. Kaczmarek, J. Ellena, L. Rozes, M. Iglesias, R. Van Deun, C. Sanchez, M. A. Monge, G. J. A. A. Soler-Illia, *Dalton Trans.* **2018**, *47*, 1808–1818.
[34] A. K. Inge, M. Köppen, J. Su, M. Feyand, H. Xu, X. Zou, M. O'Keeffe, N. Stock, *J. Am. Chem. Soc.* **2016**, *138*, 1970–1976.
[35] M. Savage, S. Yang, M. Suyetin, E. Bichoutskaia, W. Lewis, A. J. Blake, S. A. Barnett, M. Schröder, *Chem. Eur. J.* **2014**, *20*, 8024–8029.
[36] G. Wang, Q. Sun, Y. Liu, B. Huang, Y. Dai, X. Zhang, X. Qin, *Chem. Eur. J.* **2015**, *21*, 2364–2367.
[37] M. Köppen, O. Beyer, S. Wuttke, U. Lüning, N. Stock, *Dalton Trans.* **2017**, *46*, 8658–8663.
[38] A. A. Babaryk, O. R. Contreras Almengor, M. Cabrero-Antonino, S. Navalón, H. García, P. Horcajada, *Inorg. Chem.* **2020**, *59*, 3406–3416.
[39] S. M. F. Vilela, A. A. Babaryk, R. Jaballi, F. Salles, M. E. G. Mosquera, Z. Elaoud, S. Van Cleuvenbergen, T. Verbiest, P. Horcajada, *Eur. J. Inorg. Chem.* **2018**, 2437–2443.
[40] M. Feyand, E. Mugnaioli, F. Vermoortele, B. Bueken, J. M. Dieterich, T. Reimer, U. Kolb, D. de Vos, N. Stock, *Angew. Chem. Int. Ed.* **2012**, *51*, 10373–10376; *Angew. Chem.* **2012**, *124*, 10519–10522.
[41] O. Delgado-Friedrichs, M. O'Keeffe, *Acta Crystallogr. Sect. A* **2017**, *73*, 227–230.
[42] A. Noguera-Díaz, J. Villarroel-Rocha, V. P. Ting, N. Bimbo, K. Sapag, T. J. Mays, *J. Chem. Technol. Biotechnol.* **2019**, *94*, 3787–3792.
[43] Q.-X. Wang, G. Li, *Inorg. Chem. Front.* **2021**, *8*, 572–589.
[44] M. Köppen, A. Dhakshinamoorthy, A. K. Inge, O. Cheung, J. Ångström, P. Mayer, N. Stock, *Eur. J. Inorg. Chem.* **2018**, 3496–3503.
[45] V. V. Kouznetsov, C. E. P. Galvis, *Tetrahedron* **2018**, *74*, 773–810.
[46] B. Kaur, S. Chand, A. K. Malik, K. S. Dhaliwal, S. A. Younis, K.-H. Kim, *J. Cleaner Prod.* **2019**, *234*, 329–339.
[47] Deposition Numbers 2150203, 2150204, 2150208, 2150207, 2150205, 2150206, and 2179344 contain the supplementary crystallographic data for this paper. These data are provided free of charge by the joint Cambridge Crystallographic Data Centre and Fachinformationszentrum Karlsruhe Access Structures service.

Manuscript received: June 27, 2022
Accepted manuscript online: July 16, 2022
Version of record online: August 1, 2022

© 2022 The Authors. Angewandte Chemie International Edition published by Wiley-VCH GmbH